Journal of Coordination Chemistry

Spectral, structural, and superoxide dismutase activity of some octahedral nickel(II) complexes with tri-tetradentate ligands

R.N. Patel [a] , K.K. Shukla [a] , Anurag Singh [a] , M. Choudhary [a] ,
D.K. Patel [b] , J. Niclós-Gutiérrez [b] & D. Choquesillo-Lazarte [c]

[a] Department of Chemistry , A.P.S. University , Rewa 486003,
M.P., India

[b] Departamento de Química Inorgánica , Facultad de Farmacia,
Campus Cartuja, Universidad de Granada , E-18071 Granada,
Spain

[c] Lab. de Estudios Cristalográficos–IACT–CSIC , Edificio Inst. López-
Neyra, P.T. Ciencias de la Salud , Avenida del Conocimiento s/n,
E- 8100 Armilla, Granada, Spain
Published online: 20 Sep 2010.

PLEASE SCROLL DOWN FOR ARTICLE

Spectral, structural, and superoxide dismutase activity of some octahedral nickel(II) complexes with tri-tetradentate ligands

R.N. PATEL*†, K.K. SHUKLA†, ANURAG SINGH†, M. CHOUDHARY†,
D.K. PATEL‡, J. NICLÓS-GUTIÉRREZ‡ and D. CHOQUESILLO-LAZARTE§

†Department of Chemistry, A.P.S. University, Rewa 486003, M.P. India
‡Departamento de Química Inorgánica, Facultad de Farmacia, Campus Cartuja,
Universidad de Granada, E-18071 Granada, Spain
§Lab. de Estudios Cristalográficos – IACT-CSIC Edificio Inst. López-Neyra,
P.T. Ciencias de la Salud, Avenida del Conocimiento s/n, E- 8100 Armilla, Granada, Spain

Three nickel(II) complexes, $[Ni(L^1)_2] \cdot 3H_2O$ (**1**), $[Ni(L^2)_2](ClO_4)_2$ (**2**), and $[Ni(L^3)(bipy)](ClO_4)_2$ (**3**), where $L^1 = N'$-[phenyl(pyridin-2-yl)methylidene]furan-2-carbohydrazide, $L^2 = 2,6$-bis $[N,N'$-(4-methoxyphenyl)ethanimidoyl]pyridine, and $L^3 = N$-(methoxy-phenyl-pyridin-2-yl-methyl)-N-(phenyl-pyridin-2-yl-methylene)-ethane-1,2-diamine, have been synthesized and characterized by physico-chemical and spectroscopic methods. The solid-state structures of **1–3** were determined by single crystal X-ray crystallography, which revealed distorted octahedral geometry. In solid-state structure, **3** is self-assembled *via* intermolecular $\pi \cdots \pi$ stacking and intramolecular CH(methyl)$\cdots \pi$(phenyl) non-covalent interactions. Infrared spectra, ligand-field spectra, and magnetic susceptibility measurements agree with the observed crystal structures. These complexes have also been revealed to catalyze effectively the dismutation of superoxide (O_2^-) in alkaline dimethyl superoxide-nitro blue tetrazolium assay.

Keywords: Nickel(II) complexes; Single crystal X-ray analysis; Electrochemistry; Magnetic susceptibility

1. Introduction

Transition metal ions define the number of reactive sites available and modulate their activity [1]. Investigation of structural models can lead to the understanding of fundamental mechanistic aspects of enzymes as well as the development of structure–activity relationships. Chemical and physical properties of transition metal complexes may be controlled by electronic and steric factors, which may be introduced with the backbones of the ligands. Sigel *et al.* [2] reported electronic effects, such as favorable interaction between π-systems, between hydrophobic systems and between the oppositely charged side groups. These weak interactions play a crucial role in the self-organization of molecules, supramolecular chemistry, and molecular recognition [3]. Recently, nickel-containing superoxide dismutase (NiSOD) was isolated from

*Corresponding author. Email: rnp64@yahoo.co.uk

Streptomyces species [4, 5]. The enzymatic activity of NiSOD [6] is comparable to that of Cu–ZnSOD. Superoxide dismutase (SOD), which can destroy superoxide very rapidly, is nature's agent for the protection of the organism from this radical. Native SOD enzymes have been shown to exhibit protection in animal models of inflammatory diseases [7]. In a variety of scenarios, therapeutic dosage of additional SOD enzyme has shown promise, but from a number of viewpoints, namely stability, tissue permeability, oral bioavailability, specific-tissue-targeting immunogenicity; synthetic metal complexes offer considerable promise as SOD catalysts for pharmaceutical applications. SODs are an important class of redox enzymes responsible for the disproportionation of superoxide ion (O_2^-) produced by one-electron reduction of oxygen. All SODs employ two steps shown in equations (1) and (2).

$$M^{ox} + O_2^- \longrightarrow M^{red} + O_2, \tag{1}$$

$$M^{red} + O_2^- + H^+ \longrightarrow M^{red} + H_2O_2, \tag{2}$$
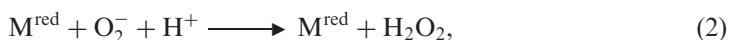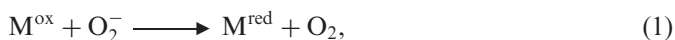
where M is the redox-active metal center capable of both oxidizing and reducing superoxide. X-ray crystallographic studies [8] of NiSODs from *Streptomyces* illustrate the nature of the enzyme-active site. In both structures, square-pyramidal coordination geometry exhibited by the Ni center in the oxidized form (NiSOD$_{ox}$) is converted to square-planar geometry in the reduced state (NiSOD$_{red}$), as the axial imidazole group derived from the His1 residue dissociates upon metal reduction. The four equatorial ligands include two thiolates from Cys2 and Cys6 in a *cis* arrangement, the deprotonated amide of the Cys2 backbone, and the N-terminal –NH$_2$ group of His1.

Synthesis and structural investigation for a series of nickel(II) octahedral complexes have been reported [9–16]. We have focused our efforts on the design of nickel(II)-based complexes as SOD mimics and have achieved success in generating stable nickel(II) complexes with outstanding catalytic SOD activity. Only a few synthetic complexes have been reported [6, 12] and these have been shown to possess modest catalytic SOD activity.

Octahedral nickel(II) complexes show relatively simple magnetic behavior. All these complexes show room temperature (RT) magnetic moment value in the range 2.84–2.97 B.M. This range depends on the magnitude of the orbital contribution. In continuation of our work [11, 12] on nickel(II) octahedral complexes, here we describe the syntheses, crystal structures, and spectroscopic characterizations of three new nickel(II) octahedral complexes namely, [Ni(L^1)$_2$]·4H$_2$O (**1**), [Ni(L^2)$_2$](ClO$_4$)$_2$ (**2**), and [Ni(L^3)(bipy)](ClO$_4$)$_2$ (**3**). We have also investigated SOD activities of these complexes.

2. Experimental

2.1. *Materials*

Nickel(II) chloride hexahydrate, sodium azide, and ammonium thiocyanate were purchased from SD fine-chemicals, India. The Schiff bases were prepared as reported [17]. All other chemicals were of synthetic grade and used as received.

2.2. *Synthesis of ligands*

Schiff bases were prepared by standard literature procedure and recrystallized from ethanol or methanol.

2.2.1. Synthesis of L^1. The ligand HL^1 was synthesized by refluxing 2-benzoylpyridine (1.832 g, 10 mmol) and 2-furoicacidhydrazide (1.261 g, 10 mmol) in ethanol for 1 h; crystals appeared immediately after cooling to RT. The crystalline solid was filtered off, washed with ethanol, and dried in air. Yield: 80%. Anal. Found (%): C, 70.02; H, 4.46; N, 14.41. Calcd (%): C, 70.08; H, 4.49; N, 14.46.

2.2.2. Ligand L^2. The ligand HL^2 was synthesized by refluxing 4-methoxyaniline (2.463 g, 20 mmol) and 2,6′-diacetylpyridine (1.832 g, 10 mmol) in ethanol for 4 h. The solution was filtered, washed with a small amount of ethanol, and allowed to stand at RT for a few days. Yield: 75%. Anal. Found (%): C, 73.84; H, 6.15; N, 11.23. Calcd (%): C, 73.89; H, 6.18; N, 11.28.

2.2.3. Ligand L^3. The ligand L^3 was synthesized by refluxing 2-benzoylpyridine (3.664 g, 20 mmol) and ethylene diamine (0.59 g, 10 mmol) in ethanol for 3–4 h. On cooling to RT, white crystalline product was filtered off and washed with methanol. Yield: 85%. Anal. Found (%): C, 76.75; H, 6.20; N, 13.26; Ni, 8.18. Calcd (%): C, 57.40; H, 4.50; N, 11.81; Ni, 8.26.

2.3. *Synthesis of complexes*

The complexes were prepared by the following general procedures:

2.3.1. [Ni(L^1)$_2$]·4H$_2$O (1) and [Ni(L^2)$_2$](ClO$_4$)$_2$ (2). To an MeOH solution (20 mL) of Ni(ClO$_4$)·6H$_2$O (0.365 g, 1.0 mmol) an MeOH solution (20 mL) of L^1 (0.582 g, 2.0 mmol) was added with stirring for 30 min at 25°C. The resulting red solution was allowed to slowly concentrate by evaporation at RT for 2 days. A red microcrystalline solid deposited was collected by filtration, washed with methanol, and stored in CaCl$_2$ desiccators at RT. Anal. Found (%): C, 58.58; H, 4.68; N, 12.01; Ni, 8.44. Calcd (%) for C$_{34}$H$_{32}$N$_6$NiO$_7$: C, 58.37; H, 4.60; N, 12.07; Ni, 8.43. FAB mass (m/z): Obs. (Calcd) 623.37 (623.37). [Ni(L^2)$_2$](ClO$_4$)$_2$ (**2**) was also prepared in a similar fashion by employing L^2 (0.75 g, 2.0 mmol) in place of L^1. Anal. Found (%): C, 54.82; H, 4.61; N, 8.21; Ni, 5.84. Calcd for C$_{46}$H$_{46}$N$_6$NiCl$_2$O$_{12}$ (%): C, 54.95; H, 4.57; N, 8.36; Ni, 5.82. FAB mass (m/z): Obs. (Calcd) 806.5 (806.5).

2.3.2. [Ni(L^3)(bipy)](ClO$_4$)$_2$ (3). To an MeOH solution (20 mL) of NiCl$_2$·6H$_2$O (0.237 g, 1.0 mmol), L^3 (0.391 g, 1.0 mmol) in MeOH solution (20.0 mL) was added with stirring for 30 min. To the above reaction mixture, a methanolic solution (20 mL) of bipy (0.156 g, 1.0 mmol) was added with stirring for 30 min at RT. After completion of reaction a light-pink microcrystalline solid deposited was collected by filtration and washed with methanol. The obtained solid was dried in air and stored in a

CaCl$_2$ desiccator. Anal. Found (%): C, 53.14; H, 4.10; N, 10.05; Ni, 7.02. Calcd for C$_{35}$H$_{34}$N$_6$NiCl$_2$O$_9$ (%): C, 53.09; H, 4.06; N, 10.00; Ni, 7.00. FAB mass (m/z): Obs. (Calcd) 638.31 (638.31).

Caution! Although no problems were encountered in this work, perchlorate salts of metal complexes are potentially explosive. They should be synthesized in small quantity and handled with great care.

2.4. *Physical measurements*

FAB mass spectra were recorded on a JEOL SX 102/DA 6000 Mass Spectrometer using xenon (6 kV, 10 mA) as the FAB gas. The accelerating voltage was 10 kV and the spectra were recorded at RT with *m*-nitrobenzoyl alcohol as the matrix. RT magnetic susceptibilities were measured by the Gouy balance using a mercury(II) tetrathiocyanato cobaltate(II) as calibrating agent ($\chi_g = 16.44 \times 10^{-6}$ c.g.s. units). Diamagnetic corrections were estimated from Pascal tables. Ligand-field spectra were recorded at 25°C on a Shimadzu UV-Vis recording Spectrophotometer UV-1601 in solution. Infrared (IR) spectra were recorded in KBr medium on a Perkin-Elmer 783 Spectrophotometer. X-band EPR spectra were recorded on a Varian E-line Century Series Spectrometer equipped with a dual cavity and operating at X-band with 100 kHz modulation frequency. TCNE was used as field marker. Cyclic voltammetry was carried out with a BAS-100 Epsilon electrochemical analyzer having an electrochemical cell with a three-electrode system. Ag/AgCl was used as reference electrode, glassy carbon as working electrode, and platinum wire as an auxiliary electrode. NaClO$_4$ (0.1 mol L^{-1}) was used as supporting electrolyte in DMSO. All measurements were carried out at 298 K under nitrogen. The solution was deoxygenated by purging nitrogen gas. The *in vitro* SOD activity was measured using alkaline DMSO as a source of superoxide radical (O$_2^-$) and nitrobluetetrazolium chloride (NBT) as O$_2^-$ scavenger [18, 19]. In general, 400 µL sample to be assayed was added to a solution containing 2.1 mL of 0.2 mol L^{-1} potassium phosphate buffer (pH 8.6) and 1 mL of 56 µmol L^{-1} alkaline DMSO solution with stirring. The absorbance was then monitored at 540 nm against a sample prepared under similar condition in DMSO (except NaOH). A unit of SOD activity is the concentration of complex, which causes 50% inhibition of alkaline DMSO-mediated reduction of NBT.

Crystals suitable for single-crystal X-ray analysis for [Ni(L^1)$_2$]·3H$_2$O, [Ni(L^2)$_2$](ClO$_4$)$_2$, and [Ni(L^3)(bipy)](ClO$_4$)$_2$ were grown from slow evaporation of the reaction mixtures at RT in CH$_3$OH : DMSO (1 : 1). Single crystals of **1**, **2**, and **3** suitable for X-ray study were mounted on a glass fiber and used for data collection. The crystal orientation, cell refinement, and intensity measurements were made using CAD-4PC performing ψ-scan measurements. Data were collected with Bruker X8 Proteum diffractometers. The data for **2** were processed with APEX2 and corrected for absorption using SADABS. The structures were solved by direct methods using SHELXS-97 [20] and refined by full-matrix least-squares against F^2 using SHELXL-97 [21]. All non-hydrogen atoms were refined anisotropically. All hydrogens were geometrically fixed and allowed to refine using a riding model.

3. Results and discussion

The nickel(II) complexes have been synthesized by the following synthetic routes:

[Ni(L^1)$_2$] (**1**)　　　　　　　　[Ni(L^2)$_2$](ClO$_4$)$_2$ (**2**)

[Ni(L^3)$_2$](ClO$_4$)$_2$ (**3**)
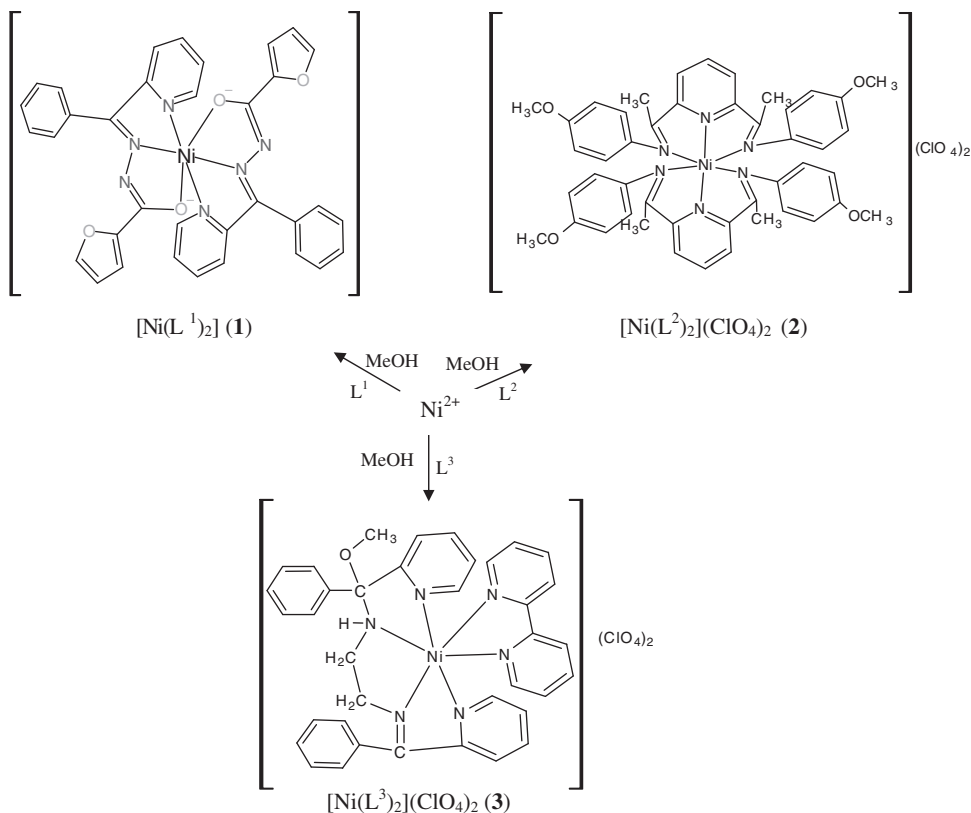
All the complexes gave satisfactory elemental analysis and were further character-ized by FAB mass spectrometry. The molar conductivity (Λ_m) measurements in 10^{-3} mol L^{-1} DMF solution show non-electrolyte [22] (11 Ω^{-1} cm^2 mol^{-1}) for **1** and a 2 : 1 electrolyte for **2** and **3** ($140 \pm 2\,\Omega^{-1}$ cm^2 mol^{-1}).

3.1. *Crystal structure*

The molecular structures of **1**–**3** are shown in figures 1–3. Crystal data and structural refinement parameters of the complexes are presented in table 1. Selected bond distances and angles are collected in tables 2–4. The nickel(II) centers are in a distorted octahedral geometry with a N$_4$O$_2$/N$_2$ donor environment. The distortions from ideal octahedral geometry about Ni are of the same extent as those commonly observed for nickel(II) complexes containing multidentate ligands [11, 12, 23]. Individual mean distances and angles compare well with those found for other octahedral nickel(II) complexes involving nitrogen donors [11, 12, 24]. The *cis* and *trans* angles (table 5)
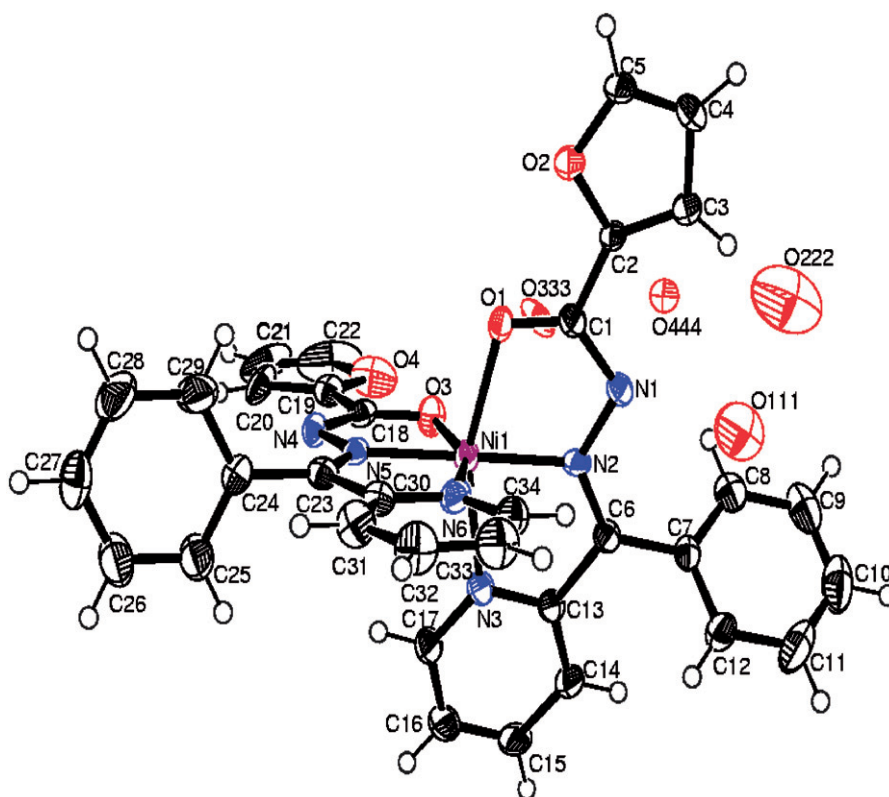
Figure 1. Projection view of $[Ni(L^1)_2] \cdot 4H_2O$ (**1**).

reflect the degree of distortion from ideal octahedral geometry. The five-membered chelate ring is planar in these complexes. These observations are comparable to those found in similar nickel(II) complexes [25].

Complex **1** crystallizes in the monoclinic space group $P2_1/n$ with four molecules in the unit cell. Nickel is in a distorted axially compressed octahedron (table 2). The two neutral ligands are tridentate *via* two pyridyl nitrogens, two hydrazone nitrogens, and two carbonyl oxygens, thus forming two fused five-membered rings. Both ligands are coordinated meridional and would be perpendicular in an idealized octahedron. However, the disposition of the ligands deviates noticeably from perpendicularity as indicated by the decreased value of the *trans* angles (N2–Ni(1)–N(5) = 178.98(18)) and by a significant difference in the values of the interligand *cis* angle associated with the same Ni–N(hydrazide) bond [102.73(14) and 101.13(16) for the angles involving the Ni–N5 and 100.11(17) and 103.60(16) for the Ni–N2 bond]. The Ni–N(hydrazide) bonds (1.982(4) and 1.984(4) Å) occupying the equatorial positions are significantly shorter than the Ni–O/N (2.075(4)–2.096(4) Å) contacts. This difference is indicated by the bis (chelating) mode of the ligands in which Ni–N (hydrazide) bonds appear to be shared by two condensed five-membered chelate rings. Such observation has been made by other workers [24, 43]. The C–N bond length in **1** (C23–N5 = 1.299(8), C18–N4 = 1.349(7), and C(1)–N(1) = 1.360(7)) is inconsistent with partial double-bond character. These factors
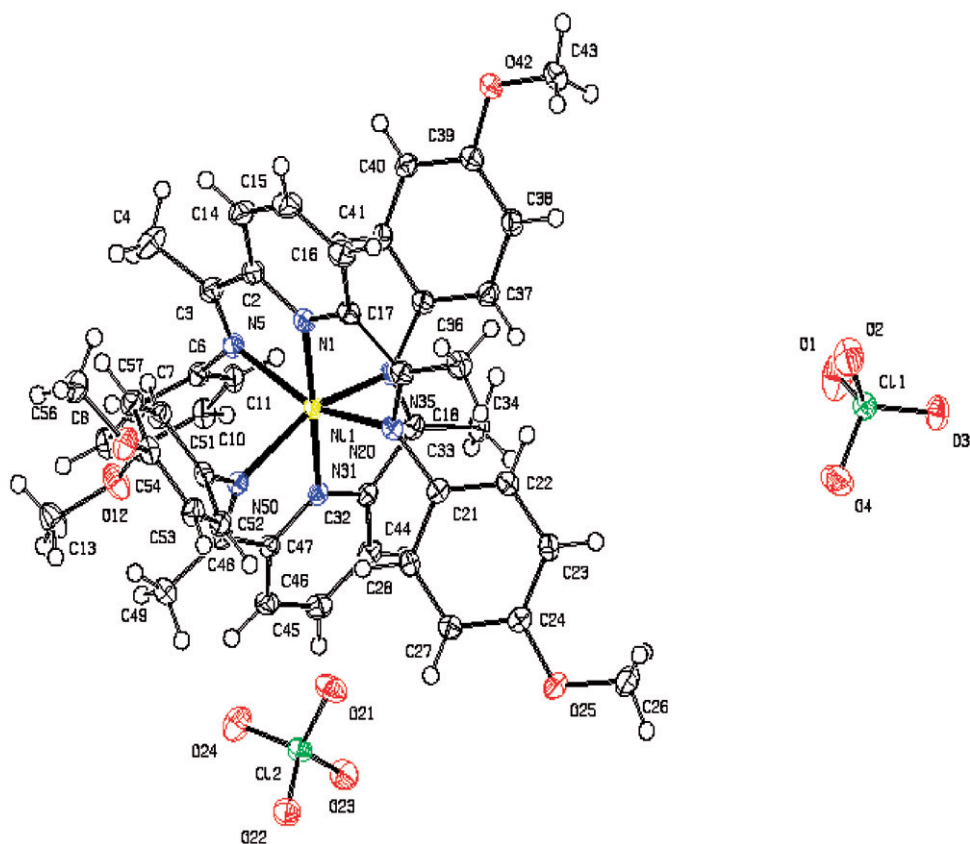
Figure 2. Projection view of $[Ni(L^2)_2](ClO_4)_2$ (**2**).

confirm coordination through the enolate form by deprotonation after enolization of the ligand. The approximate C–N bond distances of 1.32 Å, close to the value of double bond C=N (1.28 Å) [26], confirm the formation of the Schiff base [27].

Complex **2** crystallized in the monoclinic space group $P2_1/c$ with four molecules in the unit cell. Two tridentate L^2 are coordinated with nickel(II) similar to that of **1**. The nickel resides in a distorted octahedral environment comprising six nitrogens of two tridentate L^2. The Ni–N(pyridine) bonds (1.9591(4) and 1.9653(4) Å) occupying equatorial position are significantly shorter than the Ni–N (2.1136(14)–2.1311(14) Å) contacts. Again this difference (similar to that of **1**) is indicated by the bis (chelating) mode of the ligands, in which Ni–N(py) bonds appear to be shared by four condensed five-membered chelate rings and compare well with those reported for other nickel(II) complexes [28]. The C–N bond lengths of 1.28 Å [26] confirm the formation of the Schiff base [27].

In **3**, the coordination polyhedron around nickel(II) consist of atoms contributed by tetradentate L^3 and bidentate (bipy). Both ligands coordinate *via* the pyridine nitrogens, imino nitrogens, and bipyridyl imine nitrogens with a common Ni–N(py) bond.

Figure 3.   Projection view of [Ni(L^3)(bipy)](ClO$_4$)$_2$ (**3**).
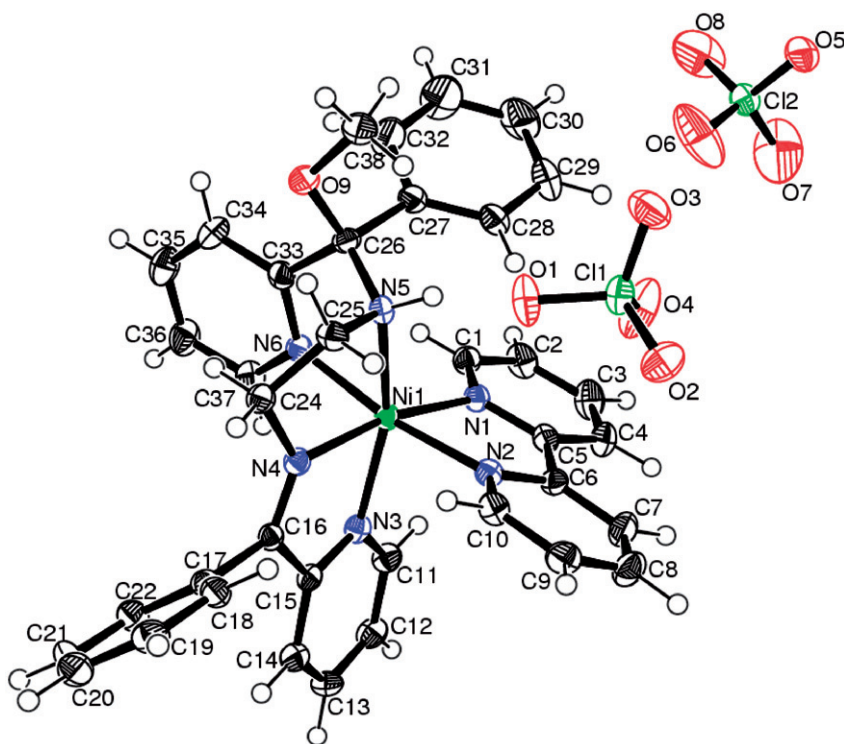
This complex crystallizes in the monoclinic space group C_2/c with eight molecules in the unit cell. The bond distances between the donor nitrogens of L^3 and metal center in the complex are Ni(1)–N(3) = 2.104(2), Ni(1)–N(4) = 2.026(6), Ni(1)–N(5) = 2.144(2), and Ni(1)–N(6) = 2.079(2) Å and bond distances of bipy and metal center are Ni–N(1) = 2.061(2) and Ni(1)–N(2) = 2.097(2) Å. Individual mean bond distances and angles within the coordination polyhedron compare well with those found in other octahedral nickel(II) complexes involving N donors [29]. *Cis* and the *trans* angles (table 5) reflect the degree of distortion from octahedral geometry. The *trans* axial sites are occupied by two nitrogens N(5) and N(3) of tetradentate L^3 (figure 3). The r.m.s deviation from planarity is in the range 0.0558–0.1526 Å. The C(16)–N(4) bond distance (1.282(2) Å) also confirm the formation of the Schiff bases, like **1** and **2**. The C(26)–N(5) bond distance of 1.473(3) Å is close to the predicted value of a single bond and also the presence of singly bonded group with C(26).

In the lattice structure of **1** all nickel(II)s form rectangular boxes when viewed along the *a*-axis with Ni–Ni distance of 9.017 and 13.696 Å, respectively. The crystal water in **1** is a single acceptor and double donor, stabilizing the network. The structures of **2** and **3** have CH···π non-covalent interactions, giving a H(14)···Cg distance of 3.296 Å in **2** and 3.208 Å in **3** (Cg is the centroid of the phenyl ring). A similar type of CH···π interaction is reported in vanadium and copper complexes of the Schiff base [30, 31]. Another significant structural observation is the intermolecular π–π stacking interaction between two individual molecules in **3**. The intermolecular stacking distance between centroids of bipy ring is 5.256 Å. A combination of coordination and weak

Table 1. Crystal data and structure refinement for **1–3**.

Empirical formula	$C_{34}H_{32}N_6NiO_8$	$C_{46}H_{46}Cl_2N_6NiO_{12}$	$C_{37}H_{34}Cl_2N_6NiO_9$
Formula weight	710.71	1004.50	836.31
Crystal system	Monoclinic	Monoclinic	Monoclinic
Space group	$P2_1/n$	$P2_1/c$	$C2/c$
Unit cell dimensions (Å, °)			
a	8.9461(3)	17.1368(17)	26.4345(6)
b	27.0834(9)	16.6817(17)	9.8187(2)
c	14.1034(4)	16.6000(18)	28.5550(7)
α	90	90	90
β	94.317(3)	109.342(4)	99.283(2)
γ	90	90	90
Volume (Å^3), Z	3407.43(19), 4	4477.6(8), 4	7314.5(3), 8
Temperature (K)	120(2)	100(2)	120(2)
D_{calcd} (mg m^{-3})	1.355	1.490	1.519
μ (mm^{-1})	0.625	2.331	0.742
Wavelength (Å)	0.71073	1.54178	0.71073
F (000)	1448	2088	3456
Crystal size (mm)	$0.32 \times 0.27 \times 0.22$	$0.15 \times 0.10 \times 0.07$	$0.23 \times 0.19 \times 0.16$
θ range for data collection (°)	2.99 to 25.00	3.81 to 66.53	3.01 to 25.00
Reflections collected/unique	31551/5993	56611/7712	30265/6443
[R_{int}]	[$R(int) = 0.0805$]	[$R(int) = 0.0492$]	[$R(int) = 0.0496$]
Completeness to θ	25.00 (99.8%)	66.53 (97.6%)	25.00 (99.8%)
Reflection used/parameters	5993/474	7712/613	6443/501
Goodness-of-fit on F^2	1.139	1.077	0.956
R_1/wR_2 (observed data)	$R_1 = 0.0774$, $wR_2 = 0.1517$	$R_1 = 0.0356$, $wR_2 = 0.0965$	$R_1 = 0.0316$, $wR_2 = 0.0700$
R_2/wR_1 (all data)	$R_2 = 0.1174$, $wR_2 = 0.1691$	$R_1 = 0.0362$, $wR_2 = 0.0971$	$R_1 = 0.0604$, $wR_2 = 0.0801$

Table 2. Selected bond lengths (Å) and angles (°) for $[Ni(L^1)_2] \cdot 4H_2O$.

Ni(1)–N(2)	1.983(4)	C(1)–N(1)	1.360(7)
Ni(1)–N(6)	2.082(4)	C(6)–N(2)	1.293(7)
Ni(1)–O(1)	2.095(3)	N(2)–C(6)	1.293(6)
Ni(1)–N(3)	2.096(4)	Ni(1)–O(3)	2.075(4)
C(23)–N(5)	1.299(8)	Ni(1)–N(5)	1.984(4)
C(18)–N(4)	1.349(7)		
N(2)–Ni(1)–N(5)	178.98(18)	N(6)–Ni(1)–N(3)	94.49(16)
N(2)–Ni(1)–O(3)	103.60(16)	O(1)–Ni(1)–N(3)	156.13(15)
N(5)–Ni(1)–O(3)	77.36(15)	O(3)–Ni(1)–N(6)	156.28(15)
N(2)–Ni(1)–N(6)	100.11(17)	N(5)–Ni(1)–O(1)	102.73(14)
N(5)–Ni(1)–N(6)	78.93(17)	N(2)–Ni(1)–N(3)	78.55(15)
N(1)–N(2)–Ni(1)	118.2(3)	N(6)–Ni(1)–O(1)	90.57(15)
N(2)–Ni(1)–O(1)	77.60(14)	O(3)–Ni(1)–O(1)	93.93(14)
N(5)–Ni(1)–N(3)	101.13(16)		

intermolecular interactions are responsible for the supramolecular architecture [32]. These non-covalent interactions are very important in crystal engineering and supramolecular frameworks [33].

3.2. *Magnetic measurement*

Magnetic moment values and electronic spectral data of the complexes are presented in table 6. The predominant contribution to the magnetic susceptibility of octahedral

Table 3. Selected bond lengths (Å) and angles (°) for $[Ni(L^2)_2](ClO_4)_2$.

Ni(1)–N(31)	1.9591(14)	Ni(1)–C(17)	1.339(2)
Ni(1)–N(1)	1.9653(14)	C(3)–N(5)	1.288(2)
Ni(1)–N(5)	2.1136(14)	C(18)–N(20)	1.292(2)
Ni(1)–N(35)	2.1226(14)	C(33)–N(35)	1.288(2)
Ni(1)–N(50)	2.1311(14)	C(48)–N(50)	1.286(2)
N(3)–Ni(1)–N(1)	177.78(6)	N(5)–Ni(1)–N(50)	86.73(5)
N(31)–Ni(1)–N(5)	100.05(5)	N(35)–Ni(1)–N(50)	115.15(5)
N(1)–Ni(1)–N(5)	77.75(6)	N(20)–Ni(1)–N(50)	100.67(5)
N(31)–Ni(1)–N(35)	77.41(5)	N(1)–Ni(1)–N(35)	103.10(5)
C(17)–N(1)–Ni(1)	119.05(11)	N(5)–Ni(1)–N(35)	98.01(5)
C(2)–N(1)–Ni(1)	118.72(11)	N(31)–Ni(1)–N(20)	104.38(5)
N(1)–Ni(1)–N(20)	77.83(5)	N(5)–Ni(1)–N(20)	155.45(5)
N(35)–Ni(1)–N(20)	85.12(5)	C(3)–N(5)–Ni(1)	114.45(11)
N(31)–Ni(1)–N(50)	77.74(5)	C(6)–N(5)–Ni(1)	120.69(10)
N(1)–Ni(1)–N(50)	101.75(5)		

Table 4. Selected bond lengths (Å) and angles (°) for $[Ni(L^3)(bipy)](ClO_4)_2$.

Ni(1)–N(4)	2.026(2)	O(9)–C(26)	1.423(3)
Ni(1)–N(1)	2.061(2)	N(4)–C(16)	1.282(3)
Ni(1)–N(6)	2.079(2)	N(4)–C(24)	1.457(3)
Ni(1)–N(2)	2.097(2)	N(5)–C(26)	1.473(3)
Ni(1)–N(3)	2.104(2)	N(5)–C(25)	1.497(3)
Ni(1)–N(5)	2.144(2)	C(16)–N(4)	1.282(3)
		C(26)–N(5)	1.473(3)
N(4)–Ni(1)–N(1)	168.30(8)	N(6)–Ni(1)–N(5)	79.21(8)
N(4)–Ni(1)–N(6)	88.81(8)	N(2)–Ni(1)–N(5)	95.09(8)
N(1)–Ni(1)–N(6)	97.47(8)	N(3)–Ni(1)–N(5)	160.02(8)
N(4)–Ni(1)–N(2)	96.51(8)	N(1)–Ni(1)–N(2)	78.43(8)
Ni(1)–N(1)–N(3)	91.90(5)	N(6)–Ni(1)–N(2)	171.69(8)
N(6)–Ni(1)–N(3)	98.18(8)	N(4)–Ni(1)–N(3)	77.38(8)
N(2)–Ni(1)–N(3)	89.23(8)	N(4)–Ni(1)–N(5)	82.74(8)
		N(1)–Ni(1)–N(5)	108.07(8)

Table 5. The *cis* and *trans* angles (°) of nickel(II) complexes.

Complex	*Cis* angle	*Trans* angle
$[Ni(L^1)_2] \cdot 4H_2O$	77.36(15)–90.75(15)	93.93(14)–178.98(18)
$[Ni(L^2)_2](ClO_4)_2$	77.41(5)–103.10(5)	155.15(5)–177.78(16)
$[Ni(L^3)(bipy)](ClO_4)_2$	77.38(8)–108.07(8)	160.02(8)–171.69(8)

Table 6. Magnetic moment and absorption maxima Dq, β, B, and $\beta°$ of 1–3 (ν_{max} in cm^{-1}).

Complex	$^3A_{2g} \rightarrow {}^3T_{2g}(\nu_1)$	$^3A_{2g} \rightarrow {}^3T_{1g}(F)(\nu_2)$	$^3A_{2g} \rightarrow {}^3T_{1g}(P)(\nu_3)$	ν_2/ν_1	Dq	β	B (cm^{-1})	$\beta°$	μ_{eff} (B.M.)
$[Ni(L^1)_2] \cdot 4H_2O$	11,050	18,200	26,310	1.65	1105	0.74	757	26.5	2.97
$[Ni(L^2)_2](ClO_4)_2$	10,200	17,860	26,300	1.75	1020	0.87	903	13	2.84
$[Ni(L^3)(bipy)](ClO_4)_2$	10,150	18,520	26,300	1.76	1015	0.92	957	8	2.89

$B = (\nu_2 + \nu_3) - 3\nu_1$; $\beta = B/B0$ [$B0$(free ion) = 1030]; $\beta° = (1 - \beta) \times 100$.

Table 7. IC_{50} values and kinetic constant of **1**, **2**, and **3**.

Complex	IC_{50} (µmol)	K_{MccF} ((mol L^{-1})$^{-1}$ s^{-1}) $\times 10^6$
$[Ni(L^1)_2] \cdot 4H_2O$	35	2.71
$[Ni(L^2)_2](ClO_4)_2$	55	1.73
$[Ni(L^3)(bipy)](ClO_4)_2$	60	1.58

K_{MccF} were calculated by $K = k_{NBT} \times$ (pH 7.8) $= 5.94 \times 10^4$ (mol L^{-1})$^{-1}$ s^{-1} [40].

Ni^{2+} complex is given by the spin-only term (equation 3):

$$\frac{3(S + 1)N\beta^2 g^2}{3kT},\qquad(3)$$

where N is Avogadro's number, β the Bohr magneton, $g = 2$ and $S = 1$. A small contribution because of spin orbit coupling between the first excited $^3T_{2g}$ and the ground state $^3A_{2g}$ leads to a magnetic moment above the spin only value [34].

The measured magnetic moment of the Ni(II) complexes at RT lies in the range 2.95–2.96 B.M. These values are in tune with a high-spin configuration and show the presence of an octahedral environment for Ni(II) in all the complexes reported in this article. These values lie within the range normally found for nickel(II) complexes [4, 10].

3.3. *Electronic spectra*

The RT electronic spectra of **1**–**3** recorded in DMSO show three absorptions [$^3A_{2g} \rightarrow {}^3T_{2g}(\nu_1)$, $^3A_{2g} \rightarrow {}^3T_{1g}(F)(\nu_2)$, $^3A_{2g} \rightarrow {}^3T_{1g}(P)(\nu_3)$], characteristics of octahedral complexes [35]. Electronic spectra of the complexes in DMSO also show a broad band around ~820 nm. This broad band seems to be an overlapping of the spin-allowed transition with the spin-forbidden transition $^3A_{2g} \rightarrow {}^3T_{1g}$. The $^3A_{2g} \rightarrow {}^3T_{1g}(P)$ band is masked by the high-intensity charge transfer band around 380 nm. Additionally, there are charge-transfer bands and intraligand transition present in the UV region for all the complexes. The ligand-field parameter Dq ($^3A_{2g} \rightarrow {}^3T_{2g}$) lowest energy transition and β (Racah parameter) values (table 6) were calculated according to the average environment rule in the range found for octahedrally coordinated nickel(II) [36].

3.4. *SOD activity*

The SOD activities for the complexes were measured. Superoxide was enzymatically supplied from alkaline DMSO and SOD activity was evaluated by the NBT assay [19, 20] following the reduction of NBT to MF^+ kinetically at 560 nm. These complexes exhibit significant catalytic activity toward the dismutation of superoxide anions. The concentration causing 50% inhibition of NBT reduction is IC_{50}. The observed IC_{50} values of the present complexes were compared with earlier reported values for nickel(II) complexes [37–40]. The catalytic activity of NiSOD [6], however, is on the same high level as that of Cu–ZnSOD at about 10^9 (mol L^{-1})$^{-1}$ S^{-1} per metal center. The IC_{50} data of the SOD activity assay along with kinetic catalytic constants of **1**–**3** [18, 41] are presented in table 7. Complex **3** shows highest SOD activity

Table 8. Cyclic voltammetric data for 1 mmol L^{-1} solution of the nickel(II) complexes in DMSO containing 0.1 mol L^{-1} NaClO$_4$ as supporting electrolytes.

Scan rate (mV s^{-1})	E_{pc} (mV)	I_{pc} (μA)	E_{pa} (mV)	I_{pa} (μA)	ΔE_p (mV)	$E^{\circ\prime}$ (mV)
[Ni(L^1)$_2$]·4H$_2$O						
	−767	1.048	−652	0.785	115	−709.5
	−783	0.795	−668	0.588	115	−725.5
[Ni(L^2)$_2$](ClO$_4$)$_2$						
100	−890	1.020	−776	0.856	114	−833
200	−895	1.920	−770	1.650	125	−832.5
[Ni(L^3)(bipy)](ClO$_4$)$_2$						
100	−782	1.048	−652	0.917	130	−717
200	−790	1.218	−670	1.044	120	−730

$\Delta E_p = E_{pa} - E_{pc}$; $E^{\circ\prime} = (E_{pa} + E_{pc})/2$.

(IC$_{50}$ = 35 μmol dm^{-3}) whereas the other two show IC$_{50}$ = 55 for **1** and 60 μmol dm^{-3} for **2**.

3.5. *Electrochemistry*

Electron-transfer properties of the complexes were studied in 10^{-3} mol L^{-1} DMSO by cyclic voltammetry. The electrochemical data for all the nickel(II) complexes are presented in table 8. Voltammograms of all complexes exhibit one-step redox in DMSO at RT under nitrogen. Voltammograms consist of two well-separated peaks, one cathodic peak potential (E_{pc}), and one anodic peak potential (E_{pa}). This reduction is quasireversible with a peak-to-peak separation of 120 ± 5 mV and the cathodic peak current (I_{pc}) is almost equal to the anodic peak current (I_{pa}). The one-electron nature of this reduction has been established by comparing its current with that of a standard ferrocene/ferrocenium couple under the experimental condition. The pertinent redox couple is represented in the following electron transfer:

$$Ni^{II} \rightleftharpoons Ni^{I}.$$
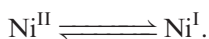
Such electrochemistry for octahedral nickel(II) complexes is earlier reported [11, 13, 28].

3.6. *IR spectra*

IR data of these complexes are compared in Supplementary material. The IR spectra show a strong band at *ca* 1600–1583 cm^{-1} characteristic of the azomethine, indicating coordination of Schiff bases through nitrogen to the metal [42]. Complex **3** displayed sharp bands at 3065 and 1555 cm^{-1} associated with ν(N–H) [43]. Complex **1** showed a stretching frequency at 1206 cm^{-1} due to ν(C–O) band and at 3433 cm^{-1} from lattice water. A broad intense band due to ClO$_4^-$ shows no splitting in **2** and **3**, indicating uncoordinated ClO$_4^-$ in both complexes. New bands at ∼500, ∼465, and 400 cm^{-1} fall in the metal-oxygen and metal-nitrogen stretching region.

4. Conclusions

We have described the synthesis and characterization of three new mononuclear nickel(II) complexes, namely $[Ni(L^1)_2] \cdot 4H_2O$ (**1**), $[Ni(L^2)_2](ClO_4)_2$ (**2**), and $[Ni(L^3)(bipy)](ClO_4)_2$ (**3**). All were structurally characterized by single crystal X-ray analysis. Complexes **2** and **3**, in the solid state, form supramolecular frameworks *via* weak intra- and inter-molecular $CH \cdots \pi$ and $\pi \cdots \pi$ stacking interactions. Magnetic moment values and spectroscopic data of these complexes show a paramagnetic nickel(II) center. Complex **3** shows higher SOD activity than **1** and **2**.

Supplementary material

CCDC 700762, 700763, and 700764 contain the supplementary crystallographic data for $[Ni(L^1)_2] \cdot 4H_2O$ (**1**), $[Ni(L^2)_2](ClO_4)_2$ (**2**), and $[Ni(L^3)(bipy)](ClO_4)_2$ (**3**), respectively. These data can be obtained free of charge *via* http://www.ccdc.cam.ac.uk/ conts/retrieving.html, or from the Cambridge Crystallographic Data Centre, 12 Union Road, Cambridge CB2 1EZ, UK; Fax (+44) 1223-336-033; or E-mail: deposit@ccdc.cam.ac.uk.

Acknowledgments

References

[1] P. Chaudhuri, K. Wieghardt. In *Progress in Inorganic Chemistry*, S.J. Lippard (Ed.), Vol. 35, p. 329, Wiley, New York (1987).
[2] P.R. Mitchell, H. Sigel. *J. Am. Chem. Soc.*, **100**, 1564 (1978).
[3] P.J. Stang, B. Olenyuk. *Acc. Chem. Res.*, **30**, 502 (1997).
[4] M.E. Stroupe, M. DiDonato, J.A. Tainer. In *Handbook of Metalloproteins*, A. Messerschmidt, R. Huber, T. Poulos, K. Weighardt (Eds), Wiley, England (2001).
[5] H.D. Youn. *Arch. Biochem. Biophys.*, **334**, 341 (1996).
[6] H.D. Youn, E.J. Kim, J.H. Roe, Y.C. Hah, S.O. Kang. *Biochem. J.*, **318**, 889 (1996).
[7] J.M. McCord. *Superoxide Dismutase*, **349**, 331 (2002).
[8] J. Wuerges, J.W. Lee, Y.I. Yim, S.O. Kang, K.D. Carugo. *Proc. Natl Acad. Sci. USA*, **101**, 8569 (2004).
[9] R. Kapoor, A. Kataria, A. Pathak, P. Venugopalan, G. Hundal, P. Kapoor. *Polyhedron*, **24**, 1221 (2005).
[10] S.M. El-Medani, O.A.M. Ali, H.A. Mohamed, R.M. Ramadan. *J. Coord. Chem.*, **58**, 1429 (2005).
[11] R.N. Patel, N. Singh, V.L.N. Gundla. *Polyhedron*, **26**, 757 (2007).
[12] R.N. Patel, M.K. Kesharwani, A. Singh, D.K. Patel, M. Choudhary. *Transition Met. Chem.*, **33**, 733 (2008).
[13] H.-B. Duan, F. Xuan, X.-M. Ren, Z.-F. Tian, L.-J. Shen. *J. Coord. Chem.*, **62**, 3772 (2009).

[14] A. Yuan, W. Liu, H. Zhou, S. Qian. *J. Coord. Chem.*, **62**, 3592 (2009).
[15] F.Y. Bai, X.T. Li, H.Y. Zhao, J. Han, Y. Xing. *J. Coord. Chem.*, **62**, 3391 (2009).
[16] A.R.M. Tawfik, M.A. El Ghamry, S.M. Abu-el-wafa. *J. Coord. Chem.*, **62**, 3377 (2009).
[17] R.N. Patel, V.L.N. Gundla, D.K. Patel. *Polyhedron*, **27**, 1054 (2008).
[18] R.N. Patel, N. Singh, K.K. Shukla, U.K. Chouhan, J. Niclós-Gutiérrez, A. Castiñeiras. *Inorg. Chim. Acta*, **357**, 2469 (2004).
[19] R.N. Patel, N. Singh, K.K. Shukla, U.K. Chouhan, S. Chakraborty, J. Niclós-Gutiérrez, A. Castiñeiras. *J. Inorg. Biochem.*, **95**, 231 (2004).
[20] G.M. Sheldrick. *Acta Crystallogr., Sect. A*, **46**, 467 (1990).
[21] G.M. Sheldrick. *SHELXL-97, Program for the Refinement of Crystal Structures*, University of Gottingen, Germany (1997).
[22] W.J. Geary. *Coord. Chem. Rev.*, **7**, 81 (1971).
[23] S.R. Elber, B.J. Helland, R.A. Jacobson, R.J. Angilicy. *Inorg. Chem.*, **19**, 175 (1980).
[24] L.P. Battablia, A.B. Corradi, L. Antolini, G. Marcotrigiano, L. Menabue, G.C. Pellacani. *J. Am. Chem. Soc.*, **104**, 2407 (1982).
[25] S. Chandra, L.K. Gupta. *Spectrochim. Acta*, **60**, 1751 (2004).
[26] J. Marsh. *Advanced Organic Chemistry, Reaction Mechanisms and Structure*, 4th Edn, Wiley, New York (1992).
[27] A.T. Chaviara, P.J. Cox, K.H. Repana, A.A. Pantazaki, K.T. Papazisis, A.H. Kortsaris, D.A. Kyriakidis, G.S. Nikolov, C.A. Bolos. *J. Inorg. Biochem.*, **99**, 467 (2005).
[28] A.K. Patra, R. Mukherjee. *Inorg. Chem.*, **38**, 1388 (1999).
[29] M.M. Morelock, M.L. Good, L.M. Trefonas, D. Karraker, L. Maleki, H.R. Eichelberger, R. Majeste, J. Dodge. *J. Am. Chem. Soc.*, **101**, 4858 (1979).
[30] P.A.N. Reddy, M. Nethaji, A.R. Chakravarty. *Inorg. Chim. Acta*, **337**, 450 (2002).
[31] S. Mandal, S.P. Rath, S. Dutta, A. Chaktavorty. *J. Chem. Soc., Dalton Trans.*, 115 (1995).
[32] P.S. Subramanian, E. Suresh, P. Dastidar, S. Waghmode, D. Srinivas. *Inorg. Chem.*, **40**, 4291 (2001).
[33] G.R. Desiraju, T. Stainer. In *Structural Chemistry and Biology*, J. John (Ed.), Oxford University Press, New York (1999).
[34] A.B.P. Lever. *Crystal Field Spectra, Inorganic Electronic Spectroscopy*, 1st Edn, p. 249, Elsevier, Amsterdam (1968).
[35] R.S. Drago, D.W. Meek, M.D. Joesten, L. LaRoche. *Inorg. Chem.*, **2**, 124 (1963).
[36] C. Cairns, S.G. McFall, S.M. Nelson, M.G.B. Drew. *J. Chem. Soc., Dalton Trans.*, 446 (1979).
[37] A. Mederos, A.M. Díaz, R. Villalonga, R. Cao. *J. Coord. Chem.*, **62**, 100 (2009).
[38] C. Wang, P. Hou, F. Bai, X. Zeng, X. Zhang, M. Ge. *J. Coord. Chem.*, **62**, 745 (2009).
[39] J.R. Anacona, D. Lorono, M. Azocar, R. Atencio. *J. Coord. Chem.*, **62**, 951 (2009).
[40] R.F. Pasternack, B. Halliwell. *J. Am. Chem. Soc.*, **101**, 1026 (1979).
[41] G. Gupta, R. Sharma, R.N. Kapoor. *Transition Met. Chem.*, **3**, 282 (1978).
[42] D.A. Stotter. *J. Inorg. Nucl. Chem.*, **38**, 1866 (1976).